SEMARAK ILMU PUBLISHING

Journal of Ship and Marine Structures

Journal homepage:
https:// semarakilmu.com.my/journals/index.php/jsms/index
ISSN: 3036 - 0137

Computational Investigation into Bilge Keel Effect on a Traditional Phinisi Boat's Resistance

Eka Suendra Putra[1,*], Eko Charnius Ilman[1], Ahmad Fitriadhy[2]

[1] Ocean Engineering Program, Faculty of Civil and Environmental Engineering, Institut Teknologi Bandung, Bandung, Indonesia
[2] Program of Naval Architecture, Faculty of Ocean Engineering Technology and Informatics, Universiti Malaysia Terengganu, Kuala Terengganu, Terengganu, Malaysia

ARTICLE INFO

Article history:
Received 4 March 2023
Received in revised form 25 March 2023
Accepted 1 May 2023
Available online 15 June 2023

Keywords:
Bilge keel; resistance; traditional boats; CFD

ABSTRACT

The paper presents the application of a passive stability system in traditional Phinisi boats equipped with bilge keels, raising concerns about potential resistance increment. Employing a Computational Fluid Dynamics (CFD) approach, the study assesses resistance values connected to bilge keel usage. The investigation focuses on the influence of bilge keel slope angles at various forward speeds. The results show an average 11% rise in total resistance with bilge keels. A comparison of baseline without bilge keel and two alternative cases of 15-degree and 25-degree angles bilge keel positions, reveals significant variations in heave and pitch conditions, resulting in a 1.87% draught reduction and 2.37% positive trim by stern. The study recommends judicious bilge keel geometry and placement to effectively manage resistance, maintaining operational safety and performance efficiency in traditional Phinisi boats.

1. Introduction

Incorporated into marine tourism operations by numerous companies, modernized traditional Phinisi boats transcend their conventional roles of transporting goods and catching marine life. A prevalent observation highlights that a significant proportion of traditional boat builders in Indonesia continue to rely solely on experiential insights, lacking a comprehensive understanding. This situation accentuates the significance of an in-depth hydrodynamic analysis of Phinisi Boat parameters, a necessity underscored by previous research [1].

The application of bilge keels as part of ship's passive stability system offers the beneficial feature of mitigating roll motion. However, this advantage is accompanied by a potential drawback – an increase in resistance under specific circumstances. To ascertain the accuracy of ship-resistance calculations, especially in scenarios involving relatively high Froude numbers, computational fluid dynamics (CFD) techniques have been harnessed. These methods involve the application of Reynolds-averaged Navier-Stokes (RANS) equations to simulate free surface effects, encompassing the generation of waves resulting from interactions between the ship and water. This approach

* *Corresponding author.*
E-mail address: ekananda_putra@polinema.ac.id

significantly enhances the precision in quantifying ship resistance, as highlighted by studies such as Suastika *et al.,* [2] and Voxakis [3].

Prior research, including the work of Liu *et al.,* [4], has employed CFD to conduct a comprehensive analysis of overall resistance in traditionally designed boats equipped with optimized bilge keels. These studies have shown a marginal increase of 1.17% in resistance. It is worth noting that such an increment may have minimal impact on high-speed vessels employing bilge keels, a notion also supported by Bhattacharyya [5]. In contrast, other study has demonstrated a more substantial 14% rise in ship resistance during tests involving the planing hull of a patrol vessel fitted with side keels [6]. Furthermore, Choi *et al.,* [7] have examined resistance and propulsion characteristics across various commercial vessels, utilizing CFD-based precision to reveal distinct drag and propulsion attributes for each vessel, thereby setting a valuable benchmark for future hull design enhancements. In a broader context, the trade-off associated with bilge keels lies in the potential increase in a ship's operational resistance. Through the implementation of an optimally designed bilge keel, the ship's resistance can be accurately gauged, with the bilge keel's configuration carefully aligned with fluid flow. Additionally, the resistance attributed to bilge keels primarily stems from frictional resistance arising due to the incorporation of augmented wetted surface areas. This insight is corroborated by the findings of Bhattacharyya [5], Lloyd [8], and Taylor [9].

This research paper presents a comprehensive computational study aimed at predicting resistance characteristics of traditional Phinisi boats. Employing the capabilities of Computational Fluid Dynamics (CFD), the investigation focuses on the assessment of total resistance (R_T) of the Phinisi boats in calm water condition. The simulation comprehensively addresses an array of influencing factors, ranging from the impact of the slope angle of the bilge keel to variations in forward speeds. The study thoughtfully considers two distinct ship scenarios: one without a bilge keel and the other incorporating a bilge keel. By utilizing CFD capabilities, this study is positioned to explore the relationship between hydrodynamics and ship design.

2. Methodology

In this chapter the existing empirical calculation and CFD method for solving a fluid flow are described to estimating resistance of the ship.

2.1 CFD Solver

The CFD solver is based on the second order finite volume method Voxakis [3] and Fitriadhy *et al.,* [10]. Acceptable boundary conditions and turbulence modeling were utilized to resolve the Reynolds-averaged Navier-Stokes (RANS) equations. Using the volume of fluid (VoF) method for generating the free surface boundary [11]

$$\frac{\partial}{\partial t}\int_V \rho \,\mathrm{d}V + \int_S \rho(\mathbf{U}-\mathbf{U}_d)\cdot\mathbf{n}\,\mathrm{d}S = 0 \tag{1}$$

$$\frac{\partial}{\partial t}\int_V \rho U_i \,\mathrm{d}V + \int_S \rho U_i(\mathbf{U}-\mathbf{U}_\mathrm{d})\,.\mathbf{n}\,\mathrm{d}S = \int_S \left(\tau_{ij}I_j - pI_i\right)\cdot\mathbf{n}\,\mathrm{d}S + \int_V \rho g_i \,\mathrm{d}V \tag{2}$$

$$\frac{\partial}{\partial t}\int_V c_i \,\mathrm{d}V + \int_S c_i(\mathbf{U}-\mathbf{U}_\mathrm{d})\,.\mathbf{n}\,\mathrm{d}S = 0 \tag{3}$$

The integral form of mass, momentum and volume fraction are given in Eq. (1), (2), and (3), respectively, where the acceleration of gravity denoted is g, the pressure is p, density of fluid is ρ, $\mathbf{U}$

is relative field velocity to stationary, $\mathbf{U}_{\mathrm{d}}$ is relative control volume velocity, S is normal vector $\mathbf{n}$ control surface, and t is time. Furthermore, the equation denotes that τ_{ij} are stresses of Reynolds, I_i is a tensor identity, and the last c_i is for volume fraction.

2.2 Prediction of Resistance

The Total resistance (R_{T}) is the combined result of total friction resistance (R_{F}) and residual resistance (R_{R}). An accumulation of shear stress to the hull surface with force working tangentially was induce by the fluid viscosity, perpendicular act by the force to produces the viscous pressure resistance (R_{VP}) and wave-making resistance (R_{W}), [12]. Formulation of resistance components are given in Eq. (4) and (5)

$$R_{\mathrm{T}} = R_{\mathrm{F}} + R_{\mathrm{R}} + R_{\mathrm{A}} \tag{4}$$

$$R_{\mathrm{T}} = R_{\mathrm{F}} + R_{\mathrm{VP}} + R_{\mathrm{W}} + R_{\mathrm{A}}. \tag{5}$$

Sources of drag for bilge keels are skin friction caused by the additional water surface and interference drag at the hull connection. To calculate drag for bilge keel, International Towing Tank Conference (ITTC) recommends the multiply the total resistance with $(S + S_{\mathrm{bk}})/S$. S represent for wetted surface area of the ship's hull, and while the wetted area of bilge keels denoted with S_{bk}. In this case, an equation is utilized for estimating the bilge keel's frictional force according to Peck [13] and Molland *et al.,* [14], is

$$D_{\mathrm{B}} = \frac{1}{2}\rho S_{\mathrm{BK}} V^2 C_{\mathrm{F}} \left[2 - \frac{2Z}{X+Y}\right] \tag{6}$$

where S is area of bilge keel wetted surface, L for average length used when calculate C_{F}. When Z approaches zero, it is presumed that interference drag equals skin friction drag [14,15].

3. CFD Simulation

This section describes the simulation creation processes, including ship particular, computation domain and boundary conditions, mesh generation, and grid independence analysis. It will be differentiated the total resistance amount while increasing the ship's speed.

3.1 Main Ship Particular

This study focuses on the traditional Phinisi boat with installed bilge keel on both side of the ship's hull. The Ship main dimension is summarised in Table 1.

Table 1
Ship particular

Description	Value
Displacement (Δ, tonnes)	76.65
Length Over All (LOA, *m*)	30.00
Length of Water Line (LWL, *m*)	20.93
Breadth (B, *m*)	5.80
Depth (H, *m*)	3.20
Draught (T, *m*)	2.00
Wetted Surface Area (WSA, m^2)	131.06
Maximum Speed (V_{max}, knots)	8.00
Block Coefficient (C_b)	0.402

3.2 Parameter Case Study

The CFD code analyse the resistance parameter of the ship by comparing the bare-hull model (BK00) to those with affixed bilge keels at 15-degree and 25-degree angles were named BK01 and BK02 models, respectively, and perform with numerous forward speeds. Table 2 and Figure 1 and 2 illustrate scenario-specific details.

Table 2
Model details of bilge keel and speed forward

Model	Ship speed (knots)		
	7.0	10.0	12.0
BK00	√	√	√
BK01	√	√	√
BK02	√	√	√

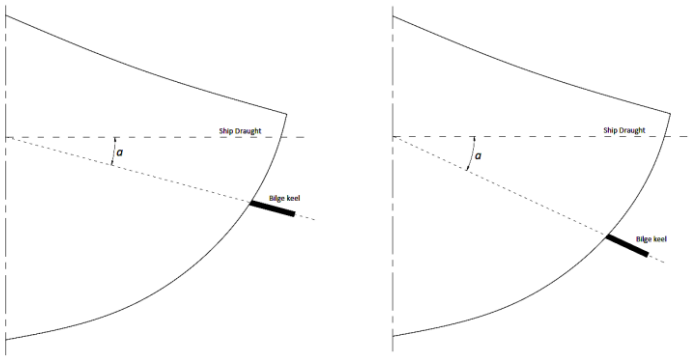

(a) (b)

Fig. 1. Bilge keel definition: (a) BK01; (b) BK02

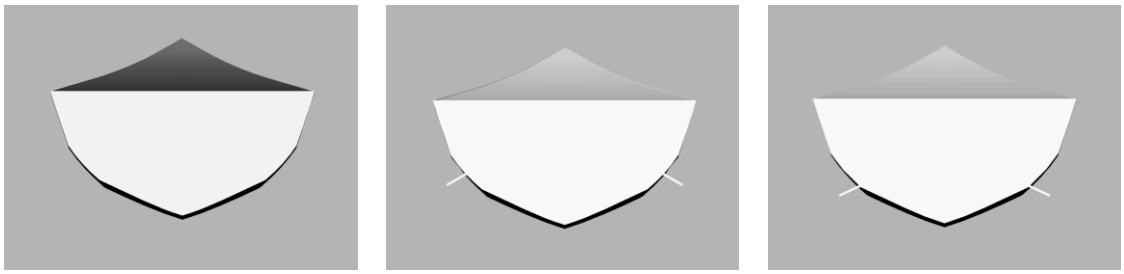

(a) (b) (c)

Fig. 2. 3-D model of hull form at mid-ship section: (a) BK00; (b) BK01; (c) BK02

3.3 Computational Domain and Boundary Condition

The computational domain configuration utilizes the initial point consist of the ratio of ship's length were summarized in Table 3. The plane of symmetry generates the centerline domain surface to precisely simulate the other half of the model. Figure 3 shows the boundary condition applied into domain.

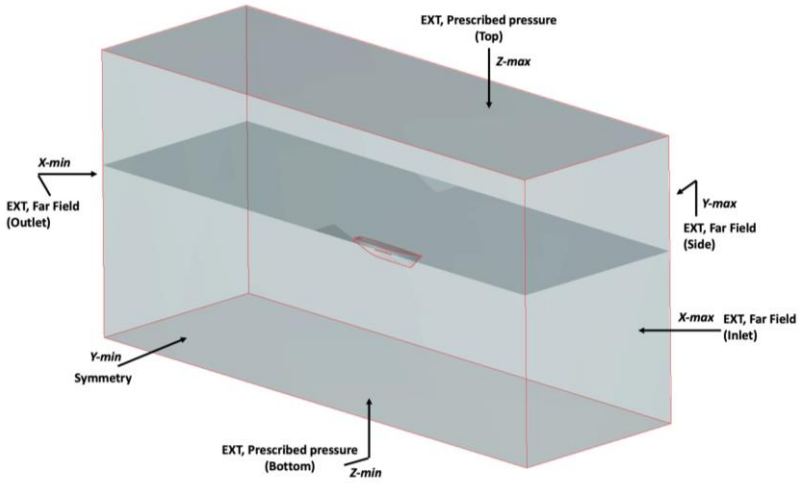

Fig. 3. Domain of computation and boundary conditions

Table 3
Domain and boundaries setup

Description	Distance of origin point	Condition	Type of domain
X-min	3.0LOA	Far field	External
X-max	1.0LOA	Far field	External
Y-min	0.0LOA	Symmetry	Mirror
Y-max	1.5LOA	Far field	External
Z-min	1.5LOA	Prescribed pressure	External
Z-max	1.5LOA	Prescribed pressure	External

To address velocity and pressure conditions, The external boundary type assigned to the computation domain is shown in Table 3. The upper and lower limits of the boundary were set as prescribed pressure. This computation has been imposed and applied for updated hydrostatic pressure at the boundary's top and bottom. To reduce computational demand and complexity, only half of the hull is displayed, as mirror type of the boundary. Moreover, solid regions were assigned as boundary conditions for the Phinisi boat model, and a wall function was applied to these surfaces.

3.4 Meshing Generation

Figure 4 represents the hexahedral meshes applied to the computational domain of the hull model. Additional local mesh refinements are applied to the internal free surface boundary to capture the waves generated by the model during computation. Around the global mesh computational domain, local box refinement was also implemented.

In this simulation, the estimated duration of every individual computation was 60 to 70 hours, utilizing 4 parallel computations with a time step value of 0.017 s on a workstation PC with Intel(R) Xeon(R) Silver 4114 T processor @ 2.20 GHz (20 CPUs), 16 gigabytes of memory (RAM), and a 64-bit operating system. The grid independence study was also performed to determine the sensitivity of

mesh numbers against reasonable values. The grid independence study will be detailed in Section 3.5.

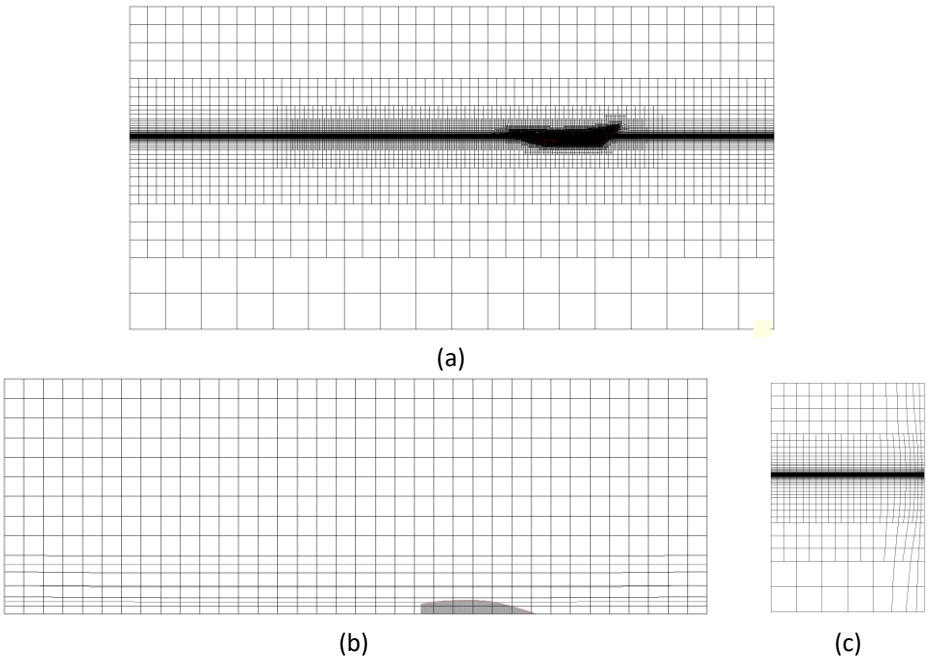

Fig. 4. Mesh generation into computational domain: (a) side view; (b) top view; (c) front view

3.5 Grid Independence Study

In order to obtain accurate results with reasonable computation time, a grid independence study has been performed, with a reference case with a ship speed of 9 knots. Increasing the number of mesh cells in every simulation, the percentage error is calculated, as suggested by Suastika *et al.,* [2] and Ariesta *et al.,* [12]. The results of those simulations are detailed in Figure 5 and Table 3.

Table 3
Various computational case for sensitivity value

Run number	Number of cells x 10^6	R_T (N)
1	0.5	7146.311
2	1.0	6966.384
3	2.0	6887.445
4	3.0	6833.943
5	4.0	6824.332

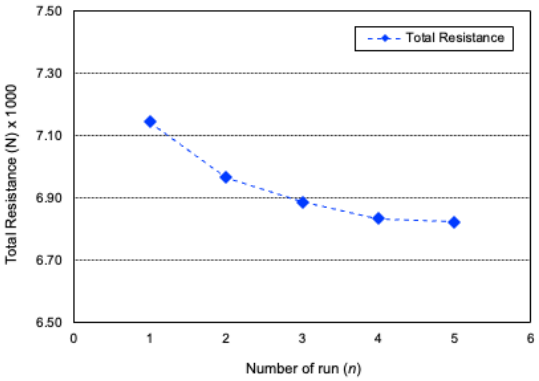

Fig. 5. Grid independence study

As shown in Figure 5 and Table 3, the total resistance decreased monotonically while number of cells used in simulation increased. Among the results, the n = 4 run number where 3.0 x 106 approximate cells were used for this computation, with a sensitivity that unsignificant affect the ship resistance results.

4. Results and Discussion

Utilizing the CFD method, this study examined ship resistance under different bilge keel conditions. Ship resistance correlates directly with speed; higher speed leads to increased resistance. The study analyzes the impact of adding bilge keels to the hull, finding that the increase in resistance is insignificant at low speeds [6] but significant at high speeds. Therefore, optimizing bilge keel design is essential to mitigate resistance effects [4]. The results of the resistance investigation are detailed in this section.

As observed in Figure 6, varying ship speeds lead to observable differences in wave height. The configuration of the ship's hull adds another layer of influence to the resulting wave height, thereby playing a role in the subsequent increase in ship resistance. By comparing hulls with and without bilge keels, as depicted in Figure 7, distinct resistance values come to light. Particularly noteworthy is the comparison of models BK01 and BK02 to the baseline scenario BK00, revealing a substantial 36% (BK01) and 11.6% (BK02) increase in total average resistance under both bilge keel conditions. This contrast becomes even more pronounced at elevated speeds, where the total resistance experiences a marked upsurge. In the context of this investigation, a deeper exploration of the sinkage and trim phenomena will contribute to a more comprehensive understanding.

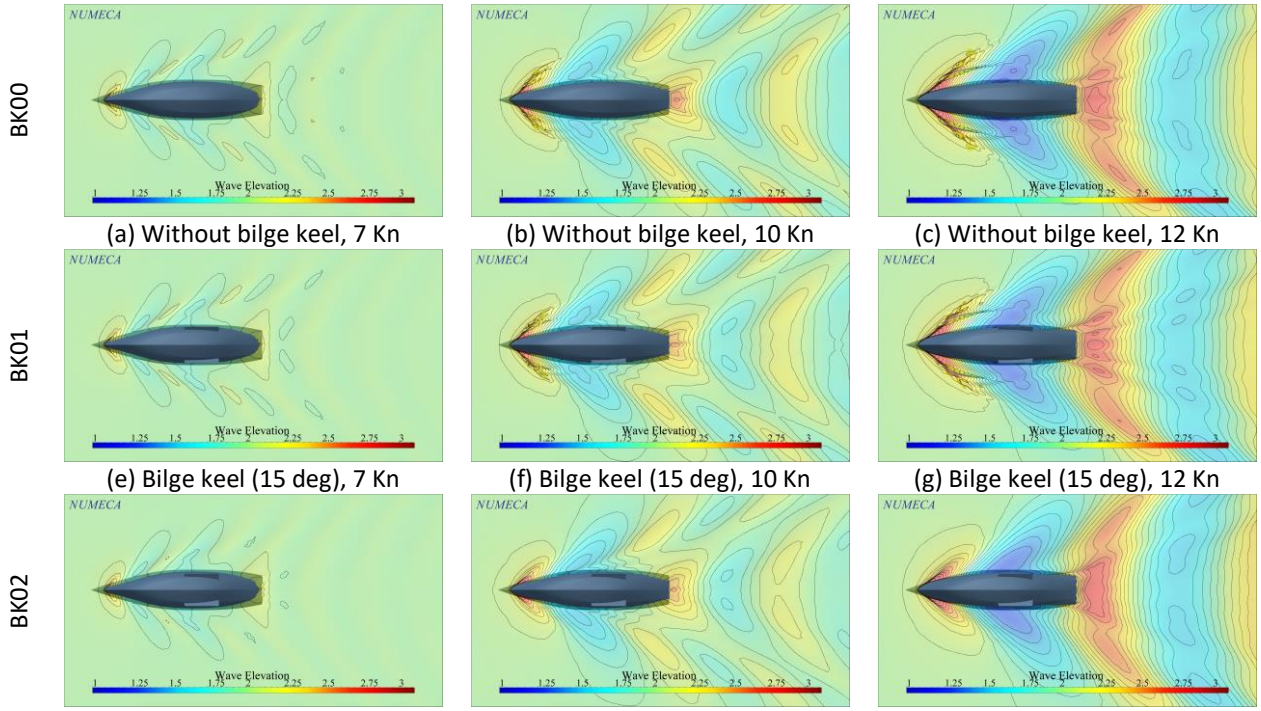

(a) Without bilge keel, 7 Kn (b) Without bilge keel, 10 Kn (c) Without bilge keel, 12 Kn

(e) Bilge keel (15 deg), 7 Kn (f) Bilge keel (15 deg), 10 Kn (g) Bilge keel (15 deg), 12 Kn

(h) Bilge keel (25 deg), 7 Kn (i) Bilge keel (25 deg), 10 Kn (j) Bilge keel (15 deg), 12 Kn

Fig. 6. Characteristic wave pattern around Phinisi ship at w/o bilge keel

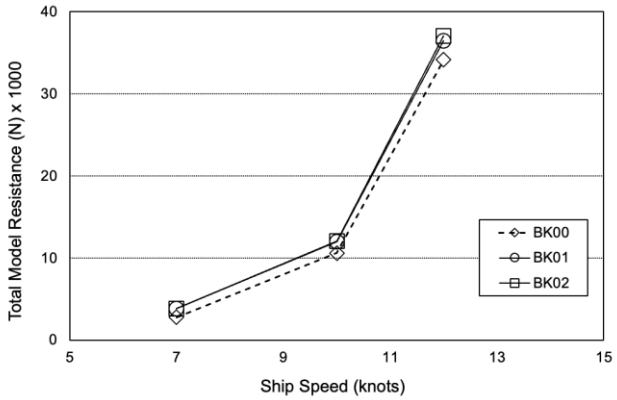

Fig. 7. Total ship resistance between bilge keel conditions with numerous speeds

Figure 8 shows the results of the heave and pitch motion characteristics. This investigation analyzed the ship's heave and pitch motions across various speeds, revealing interesting insights. Notably, when comparing models BK00 with BK01 and BK02 in terms of heave motion, BK01 exhibited an average reduction of up to 1.43%, while BK02 showcased a more substantial reduction of 2.31%. Contrarily, the investigation into pitch motion unveiled a distinct pattern. Models BK00 and BK01 demonstrated a noticeable positive increase in pitch, approximately measured at 1.2 x 10-4 rad. Furthermore, the comparison of model BK02 to BK00, at a speed of V3 = 12 knots, resulted in a minor pitch variation of merely 1.2 x 10-4 rad or a modest 2.38% increase from BK00's pitch motion value. This insightful analysis enriches our understanding of the ship's behavior across diverse conditions.

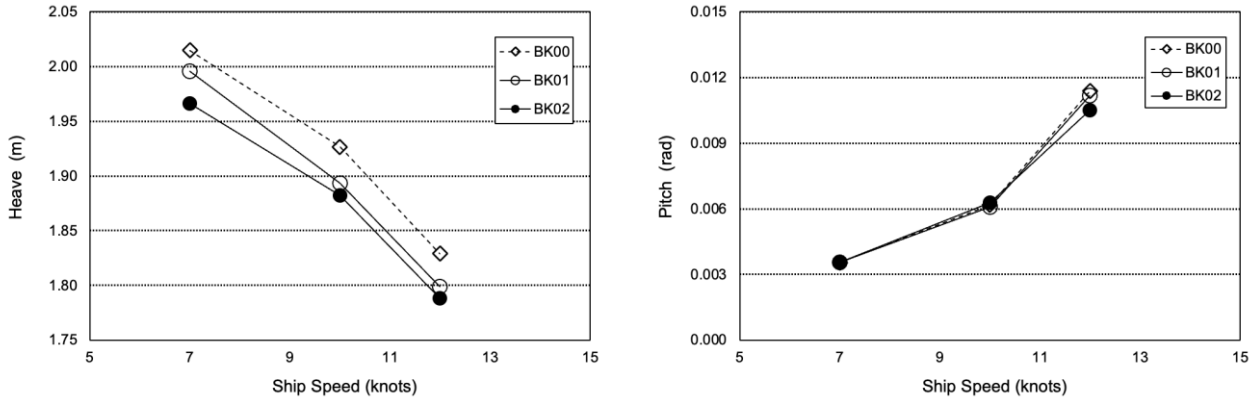

Fig. 8. Heave (left figure) and pitch motion (right figure) at various of ship's speed, V_1 = 7 knots, V_2 = 10 knots, and V_3 = 12 knots

5. Conclusions

Utilizing a rigorous CFD approach, this study extensively examines the impact of bilge keels on the resistance of Phinisi boats, encompassing a meticulous comparison between vessels with and without these appendages, as well as variations in slope angles. Notably, the presence of bilge keels emerges as a significant factor contributing to an increase in overall ship resistance, evidenced by an 11% average total ship resistance rise when contrasting the BK00 model with the BK01 and BK02 models. Furthermore, the investigation extends to analyze heave and pitch conditions, revealing promising enhancements of 1.87% and 2.37% on average, respectively, for the BK01 and BK02 models, underscoring the potential benefits of bilge keel integration. Recognizing the substantial impact of bilge keels on rolling motion, this study emphasizes the necessity for further research dedicated to effectively incorporating these appendages into the design of traditional Phinisi boats, with the potential to uncover optimized principles for bilge keel placement, thereby enhancing ship hydrodynamics and overall performance.

Acknowledgement

The authors wish to express a gratitude to Universiti Malaysia Terengganu for granting the use of Numeca Fine Marine, P.T. Perama Swara Tour & Travel for supplying the ship data model, and for the assistance provided through research funding from the Research, Community Service, and Innovation Program (P2MI) at Institut Teknologi Bandung.

References

[1] Johny, Malisan, M. Y. Jinca, Parung Herman, and Saleng Abrar. "Traditional Shipping Transport Safety Case Study: Phinisi Fleet."

[2] Suastika, IK, AF Fauzi, AS Saputra, IKAP Utama, A Firdhaus, and M Hariadi. 2021. "Benchmark Tests Of FINE/Marine CFD Code for The Calculation of Ship Resistance at High Froude Numbers." *In Proceedings of International Conference Royal Institution of Naval Architects*, pp. 106-112, 2021.

[3] Voxakis, Petros. "Ship hull resistance calculations using CFD methods." PhD diss., Massachusetts Institute of Technology, 2012.

[4] Liu, Wendi, Yigit Kemal Demirel, Eko Budi Djatmiko, Setyo Nugroho, Tahsin Tezdogan, Rafet Emek Kurt, Heri Supomo, Imam Baihaqi, Zhiming Yuan, and Atilla Incecik. "Bilge keel design for the traditional fishing boats of Indonesia's East Java." *International Journal of Naval Architecture and Ocean Engineering* 30 (2018): 1e16.

[5] Bhattacharyya, Rameswar. "Dynamics of marine vehicles." *(No Title)* (1978).

[6] Maimun, A., A. Priyanto, K. S. Wong, M. Pauzi, and M. Rafiqul. "Effects of side keels on patrol vessel safety in astern waves." *Ocean engineering* 36, no. 3-4 (2009): 277-284.

[7] Choi, J. E., K-S. Min, J. H. Kim, S. B. Lee, and H. W. Seo. "Resistance and propulsion characteristics of various commercial ships based on CFD results." *Ocean engineering* 37, no. 7 (2010): 549-566.
[8] Lloyd, A. R. J. M. "Seakeeping: ship behaviour in rough weather." *Admiralty Research Establishment, Haslar, Gosport, Publisher Ellis Horwood Ltd, John Wiley & Sons, ISBN: 0 7458 0230 3* (1989).
[9] Taylor, David W. *The speed and power of ships*. BoD–Books on Demand, 2013.
[10] Fitriadhy, A., N. S. Razali, and N. AqilahMansor. "Seakeeping performance of a rounded hull catamaran in waves using CFD approach." *Journal of Mechanical Engineering and Sciences* 11, no. 2 (2017): 2601-2614.
[11] Hirt, Cyril W., and Billy D. Nichols. "Volume of fluid (VOF) method for the dynamics of free boundaries." *Journal of computational physics* 39, no. 1 (1981): 201-225.
[12] Ariesta, Rizky Chandra, M. H. N. Aliffrananda, S. Riyadi, and I. K. A. P. Utama. "An Investigation into the Justification of the Service Speed of Ro-Ro Ferry with Block Coefficient 0.8 Based on the Resistance and Seakeeping Performance." In *Proceeding of International Conference Royal Institution of Naval Architects. no. November*, pp. 19-20. 2021.
[13] Peck, R. W. "The determination of appendage resistance of surface ships." *Admiralty Experiment Works, Haslar, AEW Technical Memorandum 76020* (1976).
[14] Molland, Anthony F., Stephen R. Turnock, and Dominic A. Hudson. *Ship resistance and propulsion*. Cambridge university press, 2017.
[15] Johny, Malisan, M. Y. Jinca, Parung Herman, and Saleng Abrar. "Traditional Shipping Transport Safety Case Study: Phinisi Fleet."